We are IntechOpen, the world's leading publisher of Open Access books Built by scientists, for scientists

4,800
Open access books available

122,000
International authors and editors

135M
Downloads

Our authors are among the

154
Countries delivered to

TOP 1%
most cited scientists

12.2%
Contributors from top 500 universities

CLARIVATE ANALYTICS BOOK CITATION INDEX INDEXED

WEB OF SCIENCE™

Selection of our books indexed in the Book Citation Index in Web of Science™ Core Collection (BKCI)

Interested in publishing with us?
Contact book.department@intechopen.com

Numbers displayed above are based on latest data collected.
For more information visit www.intechopen.com

6

A rotor model with two gradient static field shafts and a bulk twined heads system

Hitoshi Ozaku
Railway Technical Research Institute
Japan

1. Introduction

The noncontact high speed rotor is one of dream for many engineers. There are many investigations. At example, one is the bearing less motor, another is flywheel using the bulk high temperature superconducting (HTS). The bearing less motor is needed the high technical knowledge and the accurate system. HTS materials are effectively utilized to the flywheel which needs the grater levitation force, to the motor of the ship which needs the grater torque, and to the motor for the airplane which needs the grater torque and smaller weight. It is very difficult that the rotor of the micro size type generator generates a high power which rotating in a high speed.

Fig. 1. View of the original rotor model in 2007

As my first try in 2006, a small generator in which only one HTS bulk (47mm in diameter) was arranged was tested for the levitation force, but it was useless as the synchronous generator because of being unstable. And an axial gap type rotor improved to a new rotor with two gradient static field shafts which is lifted between a set of the magnets and a trapped static magnetic field of a HTS bulk. Furthermore, the improved rotor was so

rearranged as to form a twin type combination of two bulks and two set of magnets components (Figure 1). The concept of magnetic shafts which plays a role of the twined the magnetic bearing was presented, and acts as magnetic spring.
For achieve the system which achieve the more convenient and continuously examinations without use of liquid nitrogen, we fabricated bulk twined heads type pulse tube cryocooler based on the above experimental.
And, I reported [1] that this system recorded at 2,000 rpm. Later, the improved system and rotor recorded at 15,000 rpm.

2. System

2.1 Rotor model with two gradient static field shafts

The rotor is 70mm in diameter, 70mm in height, and consists of many size acrylic pipes of various sizes. A set of the combined magnets consist of both a cylindrical magnet, 20mm in diameter, 10mm in thickness, and 0.45T, and the two ring magnets, 30mm in inside diameter, 50mm in outside diameter, 5mm in thickness, and 0.33T. The cylindrical magnet was arranged to be the opposite pole in the centre of a ring magnet. The dissembled drawing of the rotor is shown in figure 2. The detail of the structure of the rotor is shown in figure 3. The centre ring part of the rotor is rotary mechanism part, and it can change easily another differ type ring.
The magnetic distribution of a set of the magnets of the rotor measured by the Hall generator with gap 0.5mm is shown in figure 4. In advance the trapped field distribution of the supplied HTS bulk was measured with Hall generator at 0.5mm above the surface of the bulk at over 1.5T field cooling. The peak value was at 0.9T. The relationship of the distributions between the magnetic distribution of the rotor and the magnetic distribution of a HTS bulk trapped in field cooling using liquid nitrogen by the permanent magnets of the rotor is shown in figure 5. The shown values of the magnetic flux density of a HTS bulk in figure 5 were reverse pole. The magnetic distributions of the both poles of the magnets of the rotary mechanism part (8 poles, acrylic ring, in figure 3 and 9) of the rotor were shown in figure 6. The x-axis is shown at vertical direction, and 0 point in x-axis is shown the hole position the acrylic ring of the rotary mechanism part of the rotor.

Fig. 2. View of the rotor model

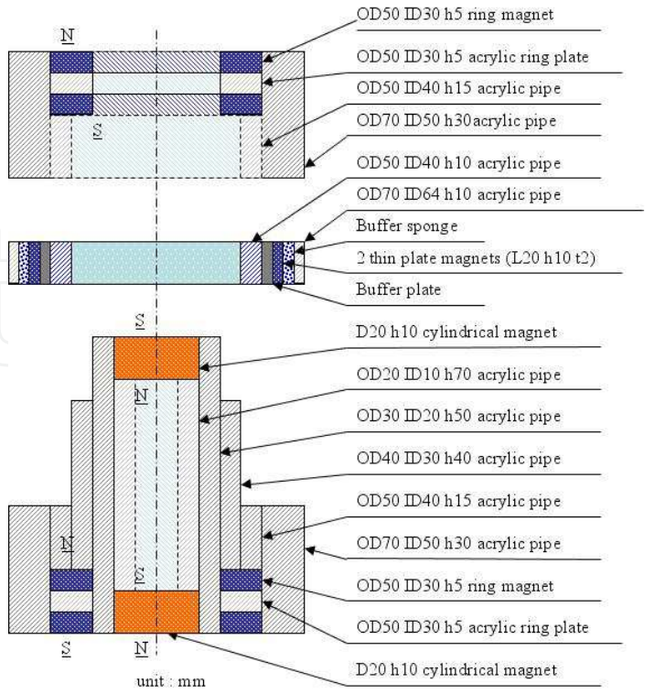

Fig. 3. Detail of component of the rotor model

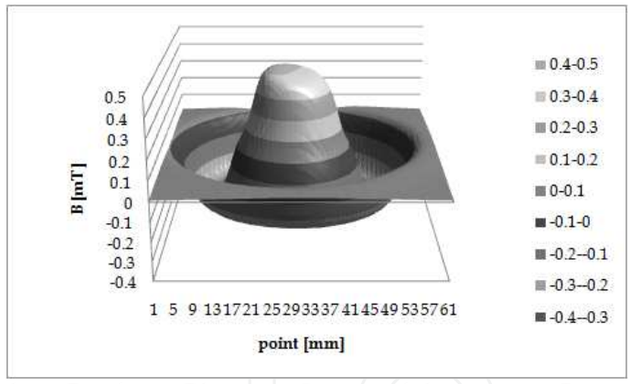

Fig. 4. Magnetic distribution of a set the component of the permanent magnets of the rotor

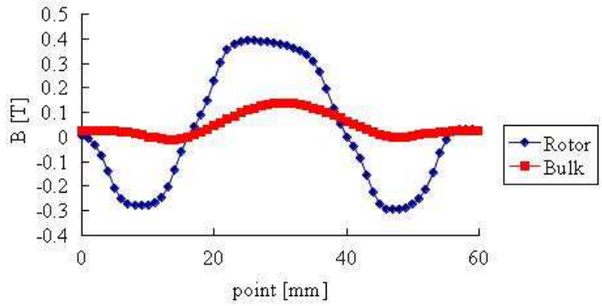

Fig. 5. Magnetic flux density of a set the component of the permanent magnets of the rotor and a trapped HTS bulk

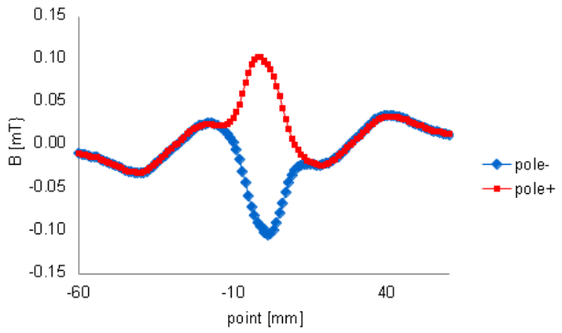

Fig. 6. Magnetic flux density of a rotary mechanism part of the rotor model

2.2 Bulk twined heads pulse tube cryocooler

We improved a pulse tube cryocooler (SPR-05, AISIN SEIKI CO., LTD.). Namely, the two bulks were installed on the boxes of a head part (Thermal Block CO., LTD.) of a pulse tube cryocooler. Figure 7 shows the schematic design of the bulk twined heads pulse tube cryocooler. The rotor explained above was set between the bulk twined heads of this cryocooler. The frost did not occur at the surface of this head in the air because the insulated space in the head was in vacuum condition, and the cold HTS bulk insulated the head. This condition was able to rotate the rotor in the air. Two sensors monitored the temperature condition. One sensor (sensor1) monitored the temperature of the cold head of the pulse tube cryocooler, and the second sensor (sensor2) monitored the temperature of the copper holder which inserted the HTS bulk in the upper head of two heads of the bulk twined heads device. Figure 8 shows efficiency of the cooler device.

After I reported [1], I tried two improvements to this device. One was that an acrylic board (W300, L300mm) with two square holes were as the sections of the top of the heads of this device, sat the bottom of the head of this device. Other improvement was that the distance between the heads of this device was expanded a few millimetres. These improvements were a key of successful to break through the unstable rotation at about 2,000 rpm. The former was because that the board cut the affect of the turbulence of the promotion gas based on the uneven face of this device. The latter was because that a point of inflexion of the relationship line between the vertical force and the vertical distance at an experiment using a HTS bulk and a permanent magnet [2].

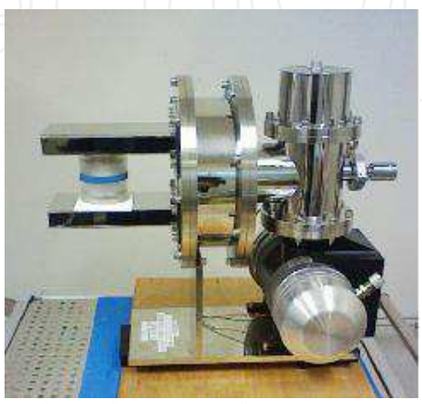

Fig. 7. The bulk twined heads pulse tube cryocooler

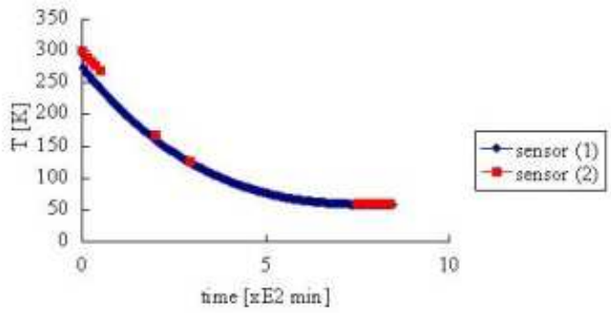

Fig. 8. The relationship between temperature of the cyocooler and time

2.3 Rotation and Measurement system

Rotation of the rotor was occurred that flow of air of the nozzles hit the wall of the holes of the rotary mechanism part of the rotor. The power generation based on action between the permanent magnets in the rotary mechanism part and the coils was used for purpose of to measurement the frequency of the rotor.

In 2007 the nozzles (1/4in, 50-100mm, stainless pipe) were connected to a nitrogen gas cylinder with silicon tubes (OD =6mm, ID =4mm). The branch of the middle from a nitrogen cylinder went in a Y-shaped joint tube (a product made in polypropylene: pp). After a nozzle was consist of a pp tube (L=48mm, ID=3mm), a pp joint (L=43mm, ID=2.5mm), a stainless steel pipe (1/4in, 300mm) (Figure 9). The nozzles were connected to an air compressor (EC1443H, Hitachi KokI Co., Ltd.) with stainless pipes (1/4in, 300mm) and silicon tube (OD =6mm, ID =4mm).and T-shaped

The frequency of the rotation was measure by the two coils connected each to the measuring instruments. There were three type coils, I-shaped coil, U-shaped coil, and T-shaped coil.

The core of the coil was used one or some pieces of the permalloy (a permalloy is alloy between iron and nickel: permability+alloy). The wire of the coil was used to having wound up copper wire OD=0.5mm. The I-shaped coil was used with core which one plate 5mm wide and 10mm long and the wire about 2m long. U-shaped and T-shaped coils were used with core which some plates 10mm wide and 50mm long and the wire about 300mm.

Centre of outer of the U-shaped and T-shaped coil fixed to the end of a stainless steel pipe (1/4in, 300mm) with the polyimide tape.

One coil of the two coils connected to a multi-meter (Type-VOAC7523, IWATSU TEST INSTRUMENTS CORPORATION) connected a PC, other coil connected to a digital oscilloscope (Type-DS-5110, IWATSU TEST INSTRUMENTS CORPORATION), stored the pulse of a coil as USB data by manual operation. The small I-shaped coil of the figure 10 was used without the U-shaped coils for confirmation of that the U-shaped coils were a little related to the rotation of the rotor.

The two nozzles were also placed by the both sides of the rotor, with the direction of the nozzles in perpendicular to the outer surface of the rotor. The U-shaped coils arranged it facing the nozzles and 90 degrees corner (in figure 9 and 10).

The states of rotation tests were taken by a video camera (Type-SR11, Sony Corporation).

The magnetic flux densities were measured by a gauss meter (Type-421, Lakeshore Cryotronics Inc.).

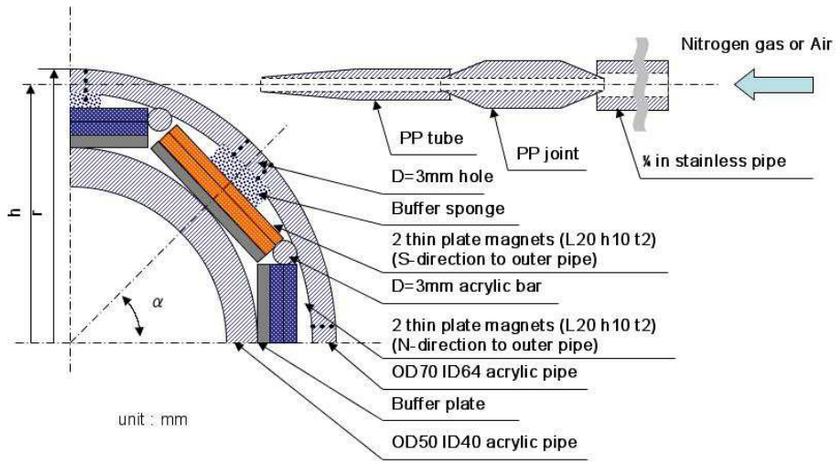

Fig. 9. Schematic drawing of the nozzle and the rotary mechanism part

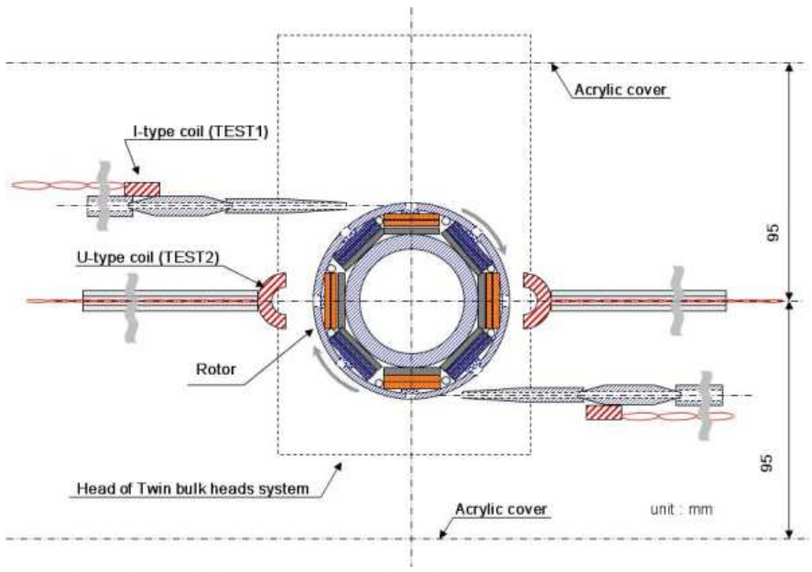

Fig. 10. Schematic drawing of the rotary mechanism part

3. Experiments and results

3.1 Original rotor model

Fig. 11. View of original rotary mechanism part

Figure 11 shows the broken original rotary mechanism part with 4 plate magnets (20mmx10mmxt2, 0.23T) were arranged in a felt disk in the central side of the cylinder to be alternate poles of the magnets for a rotary mechanism part of the rotor. This rotary mechanism part were broken at 7,770 rpm using nitrogen gas cylinder at 0.49MPa in the meter of the nitrogen gas cylinder. After acrylic boards (W300mm, L300mm) were prepared to protect or for above reason.

3.2 Improved rotor model

The rotary mechanism part was improved by acrylic ring with 8 holes (in figure 12 and 9). The both of the donut-shaped cross sections of the rotary mechanism part were needed the masking with a polyimide tape, because it was absolute terms for this rotor. The holes and sponge rubbers were also absolute terms. If the holes were changed to bucket shapes or the holes without sponge rubbers, the rotor was never rotate at 2,000 beyond. It is guessed that these holes with the sponge rubbers act as sink and source in fluid dynamics.

Fig. 12. View of the acrylic rotary mechanism part

In this examination, the acrylic cover was prepared. The box tunnel model acrylic cover (L300mm, W190mm, H82mm), was sat the between the heads of the bulk twined heads device. Inner surface of the acrylic cover top and bottom plane of the upper head of the bulk twined heads device is top of the cover off the board so that same plane. Also, inner surface of the acrylic cover bottom and top plane of the under head of the bulk twined heads device is top of the cover off the board so that same plane. This cover limited the control volume of the promote gas. The promote gas was nitrogen gas at 0.49MPa in meter of gas cylinder. The I-shaped coils were used. Purpose of this test was two. One was for confirmation of that the U-shaped coils were a little related to the rotation of the rotor. Other was for confirmation of flow around the rotor. The same examination was three times in a row. Figure 13-1 shows views of video records. The dot circle of Figure 13-1 (c) shows the hitting point of turn flow around the rotor to the inside wall (in figure 13-2). Figure 14-1 and 14-2 show the results which rotation speed and the voltage. An early stage of unstable state shown for figure 13-1 (b) suddenly stabilized it after having occurred from a rotation start from observation of a video from the back to 17 seconds for 10 seconds. The rotation fell slowly after having stopped the promote gas 10 minutes later and became an unstable state for 1010 seconds from 992 seconds. These examinations demonstrated that the U-shaped coils were a little related to the rotation of the rotor.

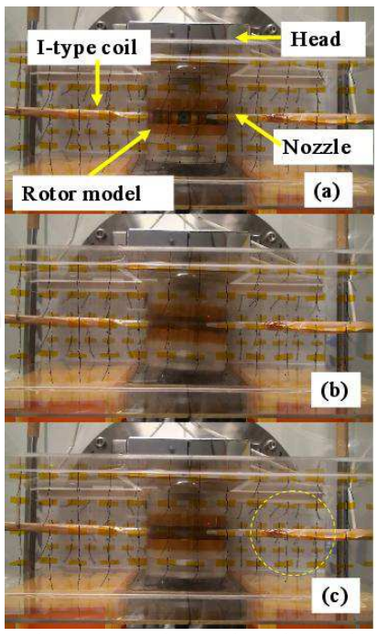

Fig. 13-1. View of test using tunnel cover, I-shaped coils and nitrogen gas

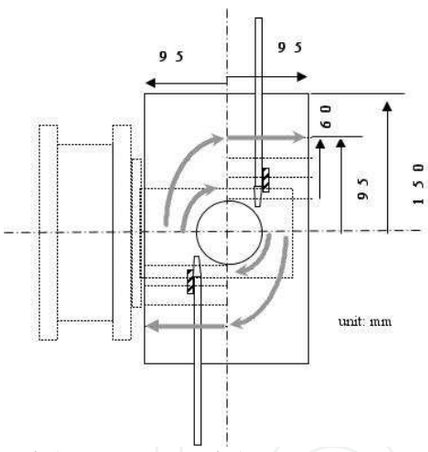

Fig. 13-2. Schematic drawing of the rotation of the test using tunnel cover, I-shaped coils and nitrogen

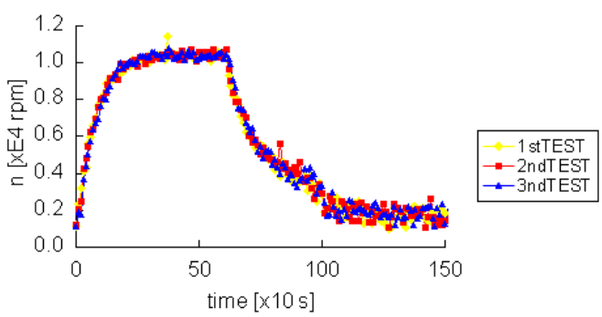

Fig. 14-1. Result of the rotation of the test using tunnel cover, I-shaped coils and nitrogen

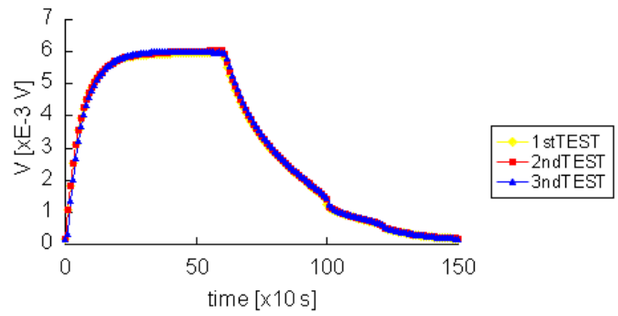

Fig. 14-2. Result of the volt of the test using tunnel cover, I-shaped coils and nitrogen

Though above the examinations show 10,000 rpm, the ability of the system as nitrogen gas cylinder was limited. At next step, an air compressor and acrylic boards of the walls without a box tunnel model acrylic cover were preparation. During the examinations the rotary mechanism part was destroyed it in 11,809 [rpm]. This result was show an ability of an increase in rotation speed under this condition.

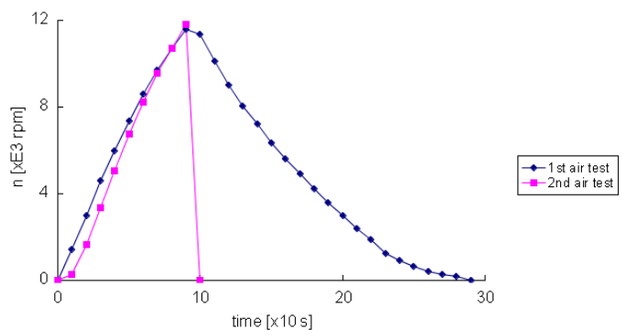

Fig. 15. Result of test of the acrylic rotary mechanism part

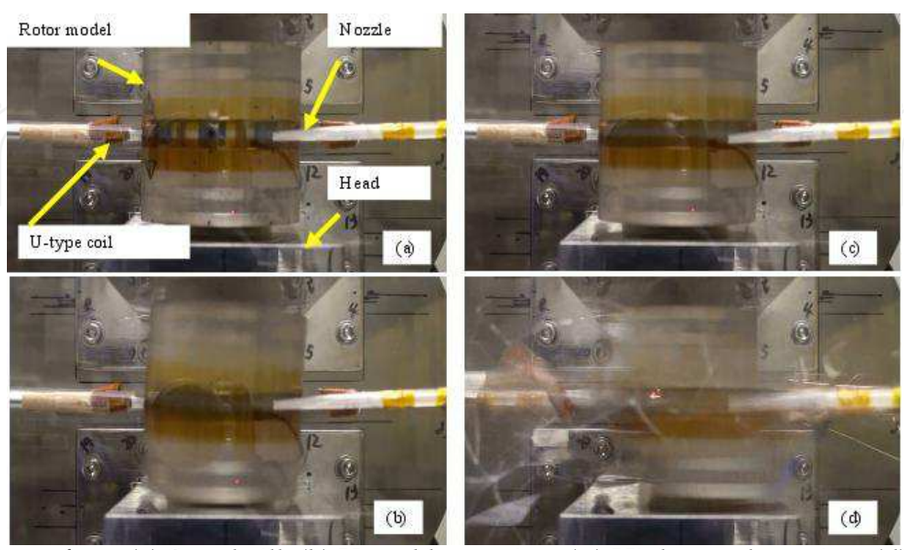

Fig. 16. View of test (a) Standstill, (b) Unstable rotation, (c) High speed rotation, (d) Broken

After the acrylic ring of the rotary mechanism part of the rotor, an aluminium ring with 8 holes was used (in figure 17). The both of the donut-shaped cross sections of the rotary mechanism part were needed the masking with a polyimide tape, because it was absolute terms. This improved rotor was used safety. In 2009, a gauss meter was join the measurement system and Hall generator was fixed to the top of the upper head of the bulk twined heads system with polyimide tape so that the centre position on the HTS bulk placed in the upper head. The promote gas was air using an air compressor at 0.2 MPa (free) in a meter of this device. The T-shaped coils were used.

Fig. 17. View of the rotary mechanism part with an aluminium ring

The result of the examinations was show that the flux flows were increase along the increase of the rotation. The results in figure 18-1 through 18-4 were show that the same examinations were ten times continuously. The vertical lines, 80x10 seconds in x-axis in figure 18-1, are shown trigger marks of the rotor completely stopped.
The results in figure 19-1 through 19-4 were show the same result using timeline. Figure 19-5 was show the result of temperature of each thermocouples, p1 was room temperature, p4 was placed at upper face of the upper head, p7 was point above the upper face of the upper head, p3 and p5 were point of the centre between the head and the end of the stainless of the nozzle, p2 and p6 were point of the end of the stainless of the nozzle. All points were along a line of centre between the nozzles.
There were shown the good repeatability except the temperature data of the HTS bulk. The gradient of a data line of the magnetic flux density was raised slowly than a data line of the rotation. The data line of the temperature was different other graphs. In figure 19-3. The temperature peaks were shown at from 3rd to 6th examinations. Though the falling of a based line of the temperature of the HTS bulk was shown along the room temperature in figure 19-5, the characteristic of the up-and-down of a base line of the temperature of the HTS bulk was also related to the rotation because another result of the test was shown in figure 20.
It is assumed to risen the magnetic flux density so that following;
Based on a point of charge (point particle) be not able to stay on a gradient of the magnetic field by Earnshaw's theory, it is assumed that a moved magnetic flux was not able to stay on a gradient of the magnetic field, and the magnetic flux pinning were moved to centre of the HTS bulk by the centripetal force, and the magnetic flux were diffused according over time, and while the temperature of the HTS bulk was down.

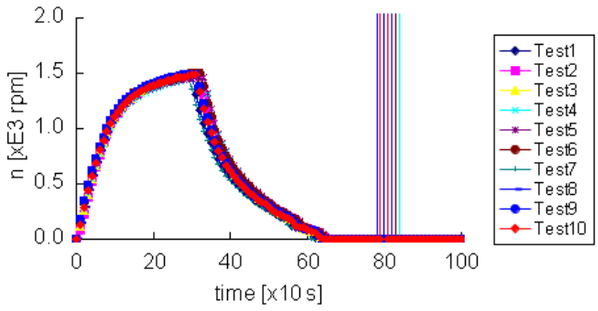

Fig. 18-1. Result of the rotation of the same tests

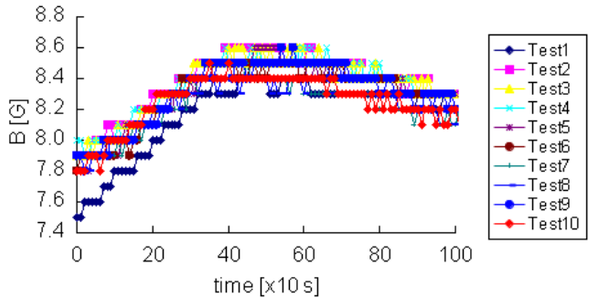

Fig. 18-2. Result of magnetic flux density of the same tests

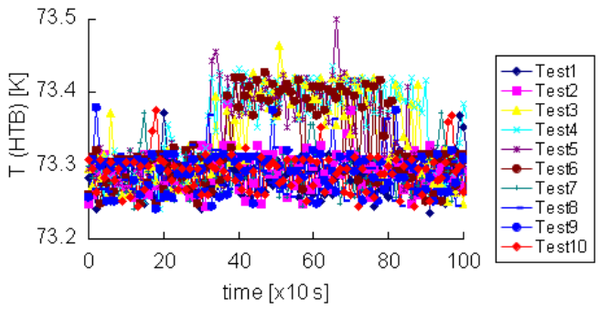

Fig. 18-3. Result of the temperature of the HTS bulk the same tests

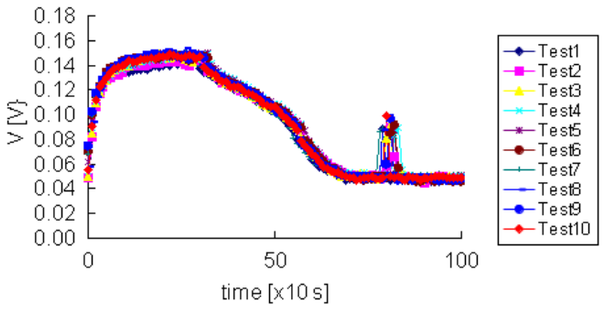

Fig. 18-4. Result of the voltage of the same tests

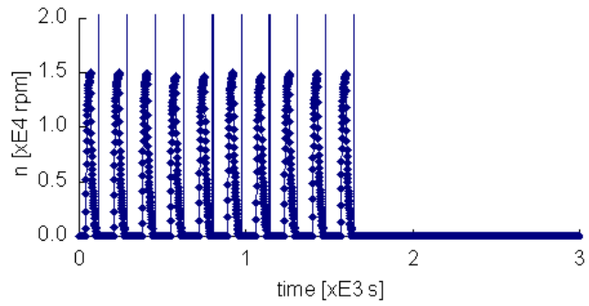

Fig. 19-1. Result using timeline of the rotation of the same tests

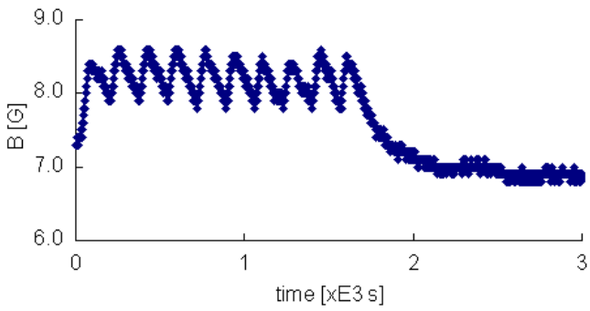

Fig. 19-2. Result using timeline of the magnetic flux density of the same tests

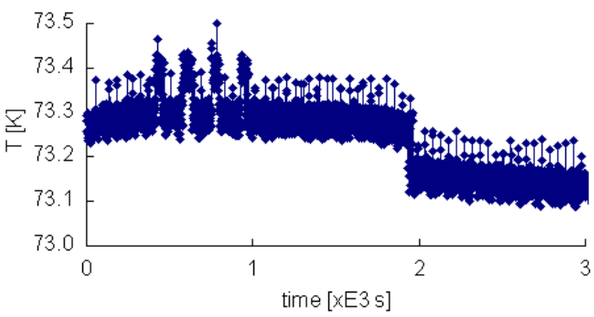

Fig. 19-3. Result using timeline of the temperature of the HTS bulk of the same tests

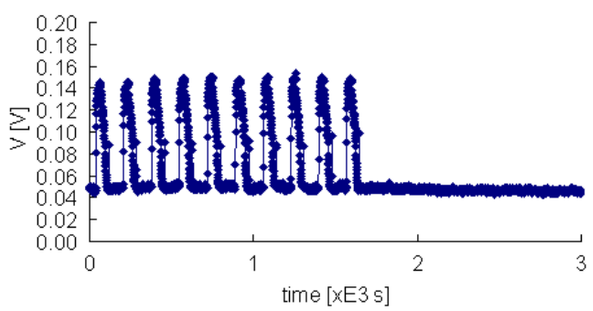

Fig. 19-4. Result using timeline of the voltage of the same tests

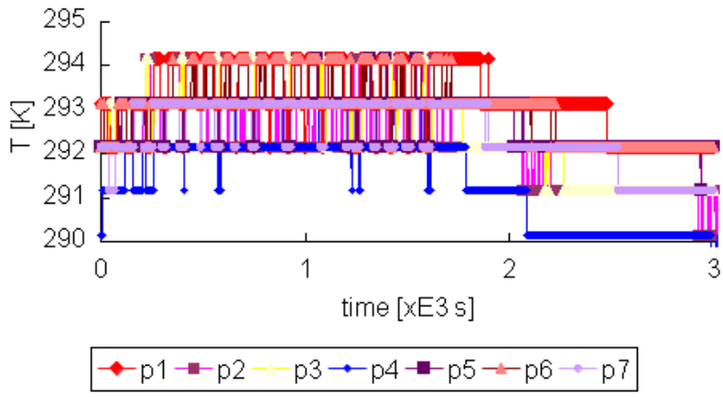

Fig. 19-5. Result using timeline of the temperature of each point around space of the system during the same tests

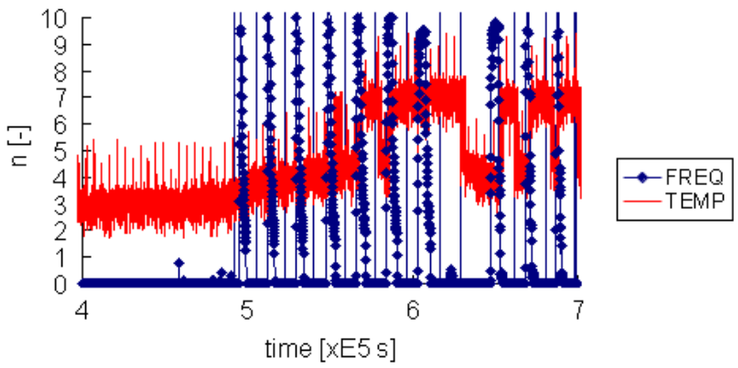

Fig. 20. Relationship between the magnetic flux density and the rotation at using timeline

In the experiment to proceed, the problem of the drag (coefficient) of the coils and nozzles was remained. There was tried the condition that differ distances between the rotor and T-shaped coils and/or the nozzles. The promote gas was air using the air compressor. The distances between the T-shaped coil and the rotor were three that near (no sign), 10mm (C10), and 15mm (C15) in figure 21. The distances between the nozzle and the rotor (see figure 9 and 10) were three that near (no sign), 15mm (N15), and 20mm (N20). The result of the test was shown in figure 21. The position of the nozzle was influenced by unstable rotation. The condition of this test was that the distance between the coil and the rotor was 10mm and the distance between the nozzle and the rotor was 15mm. In this condition, the differ pressures of the air compressor was tested (in figure 22). The condition that high pressure and long time, was not shown because the ability of the air compressor was small. The point of falling along the down slope in figure 22 was shown clearly unstable rotation. Table 1 was shown the rotation values at the point of its falling.

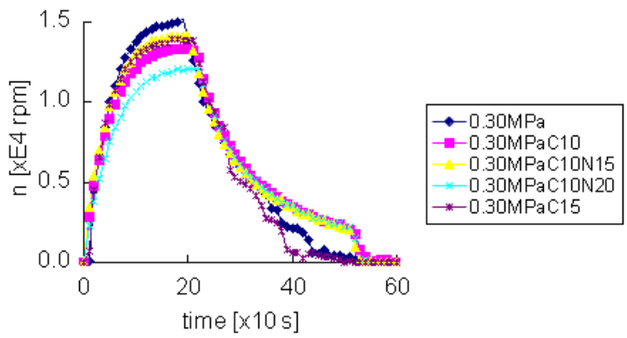

Fig. 21. Result of the rotation using the differ conditions

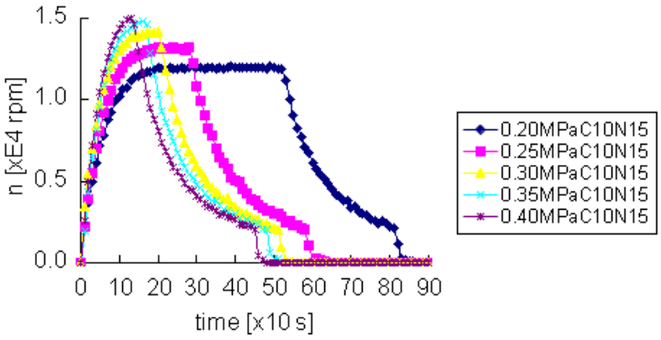

Fig. 22. Result of the rotation using the differ pressures

	0.20MPa C10N15	0.25MPa C10N15	0.30MPa C10N15	0.35MPa C10N15	0.40MPa C10N15
n [xE4 rpm]	0.2160	0.2056	0.2012	0.2027	0.2011

Table 1. The rotation values at each falling point under the differ pressures

Figure 23 was shown the data at 0.2MPa and 0.4MPa in figure 22.
The slope of the function curve line upside were legend symbol 'rev' as shown at figure 23.
In this my report, I assumed the following that;
1) The distance is the short distance in infinity in the x-axis direction as the rotation direction at around the rotor and the time is infinite.
2) The velocity of the rotor is constant while X as the external force is maxima at infinite time.
3) Though X is proportional to angular velocity, the value of X is constant.
4) The resistance of air is proportionate to the square of v.
5) Function of hyperbolic arctangent is 1 at finite time.
6) It is only problem as a contradiction between the infinite time and the finite time.
7) In this paper, it is may be no problem to formed the equation no using fluid dynamics, N-S equation, a complex velocity potential, and etc.
The equation of motion was shown to equation 1 through 3. The equation 5 is the result of that is introduced the idea of the equation (6) into the equation (4). The results of the equation were legend symbol 'cal' as shown at figure 23.

It is assumed that the true function curve line must be existed the surrounded area with a function curve line of the experiment data and a curve line of a slope of the same function curve line upside.
Therefore, it is guessed that the surrounded area with a true function curve line and a function curve line of the experiment data line shows the energy of the external force, and the surround area with a true function curve line and a curve line of the slope of the function curve line upside of the experiment data line shows the energy of the resistance of air for the rotor in this examination.

$$\frac{dv_x}{dt} = k'\mathrm{r}\omega^2 - kv_x^2 \tag{1}$$

$$\frac{dv_x}{dt} = \mathrm{X} - kv_x^2 \tag{2}$$

$$\frac{1}{v_x^2 - \frac{\mathrm{X}}{k}} dv_x = -kdt \tag{3}$$

$$\int_0^v \frac{1}{v_x^2 - \frac{\mathrm{X}}{k}} dv_x = \int_0^{\frac{1}{\mathrm{L}}} -kdt \tag{4}$$

$$v = \sqrt{\frac{\mathrm{X}}{k}} \tanh \sqrt{k\mathrm{X}} \frac{t}{\mathrm{L}} \tag{5}$$

$$\begin{pmatrix} 1 & 0 & 0 & 0 \\ 0 & 0 & 0 & 0 \\ 0 & 0 & 0 & 0 \\ 0 & 0 & 0 & \frac{1}{\mathrm{L}} \end{pmatrix} \begin{pmatrix} x \\ y \\ z \\ t \end{pmatrix} = \begin{pmatrix} x & 0 & 0 & \frac{t}{\mathrm{L}} \end{pmatrix} \tag{6}$$

	0.2[MPa]	0.4[MPa]
X [xE4 rpm]	1.2	2.2
k [-]	0.8	0.8
L [-]	100	100

Table 1. Each value in simulation

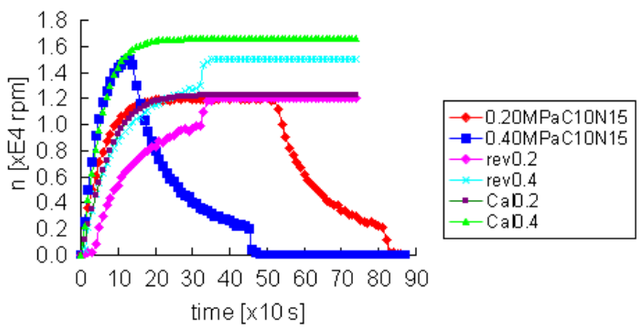

Fig. 21. Relationship between the results of the simulation and the real data

4. Conclusion

The above results of the examinations were shown the following;

1) These experimental results were demonstrated the high speed rotation.
2) It was clearly indicated the unstable rotation at 2,000 rpm.
3) The magnetic flux density was risen along that the rotation was raised. It was assumed that the magnetic fluxes were moved in direction to the centre of the HTS bulk.

5. References

H.Ozaku. (2008). A rotor model with two gradient static field shafts, *Physica C*, Vol.468, pp2125-2127

John R Hull. (2000). Superconducting bearings, *Supercond. Sci. Technol*, Vol.13, pp.1-5

Magnetic Bearings, Theory and Applications

Edited by Bostjan Polajzer

ISBN 978-953-307-148-0
Hard cover, 132 pages
Publisher Sciyo
Published online 06, October, 2010
Published in print edition October, 2010

The term magnetic bearings refers to devices that provide stable suspension of a rotor. Because of the contact-less motion of the rotor, magnetic bearings offer many advantages for various applications. Commercial applications include compressors, centrifuges, high-speed turbines, energy-storage flywheels, high-precision machine tools, etc. Magnetic bearings are a typical mechatronic product. Thus, a great deal of knowledge is necessary for its design, construction and operation. This book is a collection of writings on magnetic bearings, presented in fragments and divided into six chapters. Hopefully, this book will provide not only an introduction but also a number of key aspects of magnetic bearings theory and applications. Last but not least, the presented content is free, which is of great importance, especially for young researcher and engineers in the field.

INTECH
open science | open minds

InTech Europe
University Campus STeP Ri
Slavka Krautzeka 83/A
51000 Rijeka, Croatia
Phone: +385 (51) 770 447
Fax: +385 (51) 686 166
www.intechopen.com

InTech China
Unit 405, Office Block, Hotel Equatorial Shanghai
No.65, Yan An Road (West), Shanghai, 200040, China
中国上海市延安西路65号上海国际贵都大饭店办公楼405单元
Phone: +86-21-62489820
Fax: +86-21-62489821

IntechOpen